



Published in final edited form as:

Gastroenterology. 2012 November ; 143(5): 1319–1329.e11. doi:10.1053/j.gastro.2012.07.115.

Hedgehog Controls Hepatic Stellate Cell Fate by Regulating Metabolism

Yuping Chen¹, Steve S. Choi^{1,2}, Gregory A. Michelotti¹, Isaac S. Chan¹, Marzena Swiderska¹, Gamze F. Karaca¹, Guanhua Xie¹, Cynthia A. Moylan^{1,2}, Francesca Garibaldi¹, Richard Premont¹, Hagir B. Suliman³, Claude A. Piantodosi^{3,4,5}, and Anna Mae Diehl¹

¹Division of Gastroenterology, Department of Medicine, Duke University Medical Center, Durham, North Carolina, USA

²Section of Gastroenterology, Department of Medicine, Durham Veterans Affairs Medical Center, Durham, North Carolina, USA

³Division of Pulmonary and Critical Care Medicine, Department of Medicine, Duke University Medical Center, Durham, North Carolina, USA

⁴Department of Anesthesiology, Duke University, Durham, North Carolina, USA

⁵Department of Pathology, Duke University, Durham, North Carolina, USA

Abstract

Background & Aims—Pathogenesis of cirrhosis, a disabling outcome of defective liver repair, involves deregulated accumulation of myofibroblasts derived from quiescent hepatic stellate cells (HSC), but the mechanisms that control HSC transdifferentiation are poorly understood. We investigated whether the Hedgehog (Hh) pathway controls HSC fate by regulating metabolism.

Methods—Microarray, quantitative PCR, and immunoblot analyses were used to identify metabolic genes that were differentially expressed in quiescent vs myofibroblast HSC. Glycolysis and lactate production were disrupted in HSC to determine if metabolism influenced transdifferentiation. Hh signaling and hypoxia-inducible factor (HIF)1 α activity were altered to identify factors that alter glycolytic activity. Changes in expression of genes that regulate glycolysis were quantified and localized in biopsy samples from patients with cirrhosis, and liver samples from mice following administration of CCl₄ or bile-duct ligation. Mice were given systemic inhibitors of Hh to determine if they affect glycolytic activity of the hepatic stroma; Hh signaling was also conditionally disrupted in myofibroblasts to determine the effects of glycolytic activity.

Results—Transdifferentiation of cultured, quiescent HSC into myofibroblasts induced glycolysis and caused lactate accumulation. Increased expression of genes that regulate glycolysis required

© 2012 The American Gastroenterological Association. Published by Elsevier Inc. All rights reserved.

Corresponding Author: Anna Mae Diehl, MD, Division of Gastroenterology, Duke University Medical Center, 595 LaSalle Street, Snyderman Building, Suite 1073, Durham, NC 27710, 919-684-4173, diehl004@mc.duke.edu.

Disclosures: The authors disclose no conflicts

Author contributions: Y.C. designed and performed experiments, analyzed data, and wrote the manuscript; G.M. and C.M. performed experiments and wrote the manuscript; S.C., I.C., M.S., G.K, G.X. and R.P. performed experiments; A.M.D. designed experiments, supervised research, analyzed data, wrote the manuscript and secured funding.

Publisher's Disclaimer: This is a PDF file of an unedited manuscript that has been accepted for publication. As a service to our customers we are providing this early version of the manuscript. The manuscript will undergo copyediting, typesetting, and review of the resulting proof before it is published in its final citable form. Please note that during the production process errors may be discovered which could affect the content, and all legal disclaimers that apply to the journal pertain.

Hh signaling and involved induction of HIF1 α . Inhibitors of Hh signaling, HIF1 α , glycolysis, or lactate accumulation converted myofibroblasts to quiescent HSC. In diseased livers of animals and patients, numbers of glycolytic stromal cells were associated with the severity of fibrosis. Conditional disruption of Hh signaling in myofibroblasts reduced numbers of glycolytic myofibroblasts and liver fibrosis in mice; similar effects were observed following administration of pharmacologic inhibitors of Hh.

Conclusions—Hedgehog signaling controls HSC fate by regulating metabolism. These findings might be applied to diagnosis and treatment of cirrhosis.

Keywords

mouse model; liver disease; signal transduction; gene regulation

Introduction

Many of these MF are derived from quiescent (Q) hepatic stellate cells (HSC) via a transdifferentiation-like process whereby the cells shift from a quiescent lipogenic state to become proliferative and fibrogenic.¹ Researchers have identified a number of injury-related factors that promote HSC transdifferentiation and MF growth. Conversely, MF populations gradually involute, and fibrosis tends to regress, when injury is cured.² The global power of the microenvironment in dictating HSC fate is further supported by evidence that targeted efforts to constrain MF accumulation during active liver injury have failed. These observations suggest that redundant injury-initiated mechanisms activate the molecules that ultimately control HSC fate, and justify work to identify those master regulators.

There is emerging evidence that Hedgehog, a master developmental regulator,^{3, 4} becomes reactivated during adult wound healing.⁵ The Hh pathway is activated when Hh ligands bind to their receptor Patched (PTCH) on the surface of Hh-responsive cells. This relieves PTCH's inhibitory actions on Smoothened (SMO), the signaling competent Hh co-receptor. SMO then translocates to the cilium where it promotes the nuclear localization of the transcription factors GLI1, GLI2 and GLI3, which control the expression of Hh-target genes. Most of the biological effects of the Hh pathway are thought to result from transcriptional regulation of GLI-target genes whose products influence stem cell renewal and lineage decisions, as well as cell cycle progression and cell migration.⁶⁻⁸ Although the exact role of Hh in adult tissue repair remains somewhat obscure, the pathway seems to control critical cell fate decisions that are required for reconstruction of healthy tissue because cancers and fibrosis typically result when Hh signaling becomes deregulated.^{6, 9, 10} Inhibiting Hh signaling also blocks adipogenesis,¹¹ suggesting a role for the Hh pathway in metabolism. However, it is not known if the metabolic effects of Hh influence its other actions, or *vice versa*.

Like several of the key cell types involved in liver repair, HSC are Hh-responsive.^{6, 12} Hh pathway activation promotes transition of quiescent (Q)-HSC into MF-HSC, and pathway inhibition drives MF-HSC to revert back to a quiescent phenotype.¹³ We hypothesized that Hh signaling might direct the fate of HSC by regulating their metabolism because Q-HSC are adipocyte-like², and loss of lipid is a hallmark of Q-HSC transition to MF.^{1, 14, 15}

Materials and Methods (Full Methods available in Online Supplement)

Primary HSC studies

Primary HSCs were isolated from adult rats, wild-type C57BL6 mice, *Smo^{tm2Amc}/J* (SMO-LoxP) mice¹⁶, or mtGFP transgenic mice¹⁷ and culture-activated for up to 7 days in DMEM containing either 4500 or 1000mg/L glucose.^{18, 19} 4-day cultures were treated with

inhibitors of glycolysis (2-deoxy-glucose, Sigma-Aldrich), lactate dehydrogenase (FX11),²⁰ Smoothened (GDC-0449, Selleck Chemicals),²¹ or HIF1 α (acriflavine (ACF), Sigma-Aldrich)²² and analyzed on day 7. In HSCs from SMO-LoxP mice, Cre-recombinase adenoviral vectors were used to delete the floxed smoothened allele. Results were compared to HSCs treated with GFP adenoviral vectors.

Animal studies

C57BL/6 mice from Jackson Laboratories (Bar Harbor, ME) were used to model liver injury. All studies were approved by the Duke University Institutional Animal Care and Use Committee as set forth in the 'Guide for the Care and Use of Laboratory Animals' published by the National Institutes of Health.

Acute Liver Injury Models—CCl₄. Wild-type male mice were injected i.p. with olive oil (n=2) or CCl₄ (CCl₄:olive oil=1:20, n=6) and sacrificed on day 2, 4, or 7. **Partial hepatectomy (PH).** Adult male mice were subjected to PH and cyclophosphamide treatment as described.²³ Livers were harvested at the time of PH (n=6) or after 48h (n=6).

Chronic Liver Injury Models—BDL. Wild-type male mice underwent bile duct ligation (BDL; n=5) or sham surgery (n=4) then sacrificed after 14 days. SMO-LoxP mice¹⁶ (Jackson Laboratories) were crossed with α SMA-Cre-ERT2 transgenic mice to generate double-transgenic mice (DTG) in which tamoxifen treatment induces conditional deletion of SMO in α SMA(+) cells. Adult (8-12 weeks) mice were subjected to BDL or sham surgery (n=8 mice/group); treated with vehicle or tamoxifen on days 4, 6, 8, and 10 post-BDL; and sacrificed 14 days post-BDL. **MCD diet.** Wild-type male mice were fed control (n=2) or methionine choline deficient diets (MCD; MP Biomedicals, Solon, OH; n=3) for 8 weeks. **MDR2^{-/-} mice.** Aged (52-62 week old) MDR2^{-/-} mice were treated with vehicle (n=10) or GDC-0449 (n=10) for 9 days.²⁴

Human studies

Anonymized healthy and diseased human livers were examined for expression of glycolysis markers as per Institutional Review Board-approved protocols.

Statistical analysis

Results are expressed as mean \pm standard error mean (SEM). Analyses were performed using Student's *t*-test. *P*<0.05 is considered significant.

Results

Metabolism is reprogrammed during HSC transdifferentiation

We performed microarrays to screen HSC for transition-associated changes in metabolism. To capture early, as well as late, events in the transdifferentiation process, gene expression was compared in freshly-isolated primary HSC and HSC after 7 days in culture. This approach differed from earlier studies that examined HSC cultured 1 day or more.²⁵ We found that a significant number of the genes that are differentially expressed in Q-HSC versus MF-HSC are involved in metabolism (Supplementary Tables 1,2). This point had not been emphasized previously, and suggests that alterations in HSC metabolism occur rapidly during their transdifferentiation. The gene expression profile of MF-HSC also resembled that of highly proliferative cells.²⁶ Because proliferative cells are often glycolytic,^{26, 27} we compared glycolytic activity in Q-HSC and MF-HSC. MF-HSC demonstrated significantly increased expression of glycolytic enzymes (Fig. 1A-C, Supplementary Fig. 1A) and glucose and lactate transporters (Fig. 1D), with co-incident down-regulation of genes involved in

gluconeogenesis (Fig.1E). Notably, the most striking differences in many of these transcripts occurred within the initial 48h of culture. Hence, the metabolic shifts would have been overlooked if gene expression had been evaluated only at later time points. For example, mRNA levels of the glucose transporter, Glut1, and two key glycolytic enzymes, hexokinase (Hk)2 and pyruvate kinase (Pk)m2,²⁸ increased 6-25-fold within 6-24h in culture (Supplementary Fig.2) and remained elevated on culture day 7 (Fig.1A). Western blot and immunocytochemistry confirmed that expression of these glycolytic enzymes was rapidly switched on when Q-HSC were placed into culture, and then maintained at high levels (Fig. 1B-C). Conversely, transcripts for phosphoenolpyruvate carboxykinase (Pck)1 and fructose bisphosphatase (Fbp)1, two key gluconeogenic enzymes,²⁶ plummeted by 90% during the initial 48h in culture and remained extremely low on culture day 7 (Fig.1E).

As previously described,¹ expression of genes involved in lipid synthesis, oxidation and uptake fell by 50-90% during early HSC culture and remained low thereafter (Supplementary Fig.1C). Unlike the early and dramatic changes in metabolism-associated genes, induction of classical MF-HSC markers, such as alpha smooth muscle actin (α SMA) and collagen1 α 1, occurred between culture days 2 and 7 (Supplementary Fig.1D and 2), during which time the cells acquired the typical phenotype of proliferative MF-HSC (Supplementary Fig.1E-F). HSC cultured in high and low glucose medium demonstrated similar patterns of changes in all of the aforementioned parameters (Fig.1, Supplementary Fig.3); in both situations the kinetics suggest that major changes in HSC metabolism occur very early during the transition process and are maintained after the cells become MF.

Interestingly, we found that mRNA levels of Pdk3, which inhibits the conversion of pyruvate to acetyl-CoA,²⁶ were increased in MF-HSC (Supplementary Fig.1B), suggesting that MF-HSC divert some glycolysis-generated pyruvate towards lactate production. Indeed, HSC rapidly accumulated lactate once they were placed into culture (Fig.1F), and intracellular lactate levels remained elevated despite progressive up-regulation of mRNAs encoding the lactate export pump, MCT4 (Fig.1D). Many highly proliferative cells, including cancer cells, exhibit high glycolytic activity and produce lactate despite retaining large numbers of mitochondria and thus, the capacity for oxidative phosphorylation (i.e., aerobic metabolism). Paradoxically, cancer cell growth is dependent upon glycolysis, although glycolysis is significantly less efficient than oxidative phosphorylation for generating ATP from glucose. This phenomenon has been dubbed the Warburg effect.^{26, 28}

We used electron microscopy to determine if glycolytic, lactate-producing HSC that are transdifferentiating under aerobic conditions retain mitochondria. We noted very few mitochondria in freshly-isolated Q-HSC, whereas mitochondria were abundant in 7-day culture-activated MF-HSC (Supplementary Fig.4A). We further studied primary HSC from transgenic mtGFP-tg reporter mice in which mitochondria are marked by expression of green fluorescent protein (GFP).¹⁷ Both the numbers of GFP(+) foci/cell and the percentage of GFP(+) cells increased dramatically during the initial 72h of HSC culture (Supplementary Fig.4B), confirming that HSC retain mitochondria and hence, the capacity for oxidative phosphorylation, as they transdifferentiate into MF. The aggregate findings, therefore, indicate that HSC quickly become glycolytic and undergo a Warburg-like response as they become myofibroblastic.

Metabolic reprogramming controls HSC fate

To understand the functional significance of metabolic reprogramming in HSC, we cultured MF-HSC under standard conditions, or in 2-deoxy-glucose (2DG), to inhibit glycolysis,²⁹ and assessed effects on proliferation and gene expression. As noted in glycolytic cancer cells,²⁹ 2DG caused dose-dependent cytotoxicity in MF-HSC (data not shown). However, when cultured in low concentration of 2DG, most HSC remained viable, decreased their

proliferation, repressed expression of MF genes, re-expressed lipogenic genes, and re-accumulated lipids (Fig.2A-B). Because inhibiting glycolysis caused MF-HSC to revert to the Q-HSC phenotype, we asked if metabolic end-products themselves might control HSC fate. Glycolysis generates pyruvate, which is converted into lactate via an LDHA-catalyzed reaction.^{20, 26} Our initial studies showed that HSC accumulate large amounts of lactate as a result of metabolic reprogramming (Fig.1F). To assess the direct effects of lactate on HSC transition, we treated MF-HSC with FX11, a pharmacologic inhibitor of LDHA.²⁰ Blocking conversion of pyruvate to lactate in MF-HSC decreased the lactate:pyruvate ratio, inhibited proliferation, suppressed expression of MF-genes, and induced lipid accumulation and lipogenic genes (Fig.2C-D, Supplementary Fig.5). Critically, dose-response studies demonstrated that FX11 suppressed expression of MF markers even when added to cultures at concentrations that had no appreciable effect on cell growth (Supplementary Fig.5). Thus, to become myofibroblastic, HSC must activate glycolysis in order to accumulate intracellular lactate, indicating that metabolic reprogramming controls the fate of HSC.

Hedgehog signaling controls metabolic reprogramming to direct HSC fate decisions

Hh signaling is known to inhibit adipogenesis.¹¹ Our findings indicated that changes in HSC lipid content were secondary to activation of glycolysis and the resultant lactate accumulation. Virtually nothing has been reported about the effect of Hh signaling on carbohydrate metabolism. Therefore, we used various approaches to manipulate Hh signaling in freshly-isolated Q-HSC or culture-activated MF-HSC to determine if this influences glycolytic activity. Because glycolysis is induced within hours of HSC isolation (Supplementary Fig.2), we injected SMO-LoxP mice¹⁶ with adenoviral vectors for Cre-recombinase (or control vectors) to conditionally delete the obligate Hh signaling intermediate, *smoothed*, in Q-HSC *in vivo*. Two days later, Q-HSC were isolated and RNA was analyzed. Q-HSC from Cre-treated mice expressed less SMO mRNA than comparable cells from control mice, while mRNA levels of the Q-HSC marker, PPAR γ , were significantly increased, consistent with published evidence that HSC require Hh signaling to transdifferentiate into MF.¹³ *Smoothed* deletion in Q-HSC also further reduced their low basal mRNA expression of *glut1*, *Hk2*, and *Pkm2* (Fig.3A). Conversely, when Q-HSC from wild-type mice were treated with SAG (a direct pharmacologic agonist of *Smoothed*)³⁰ immediately upon isolation, significant augmentation of *glut1* and glycolytic gene mRNA induction occurred (Fig.3A). To determine if inhibiting *smoothed* also suppressed glycolysis in MF-HSC, 4-day culture-activated MF were treated with GDC-0449, a direct *Smoothed* antagonist,³¹ for 3 days. Inhibiting *Smoothed* in cultured MF-HSC caused dose-dependent suppression of glycolytic gene expression and MF markers (Fig.3B). In order to exclude potential off-target effects of GDC-0449, day 4 cultured HSC from SMO-LoxP mice¹⁶ were treated with adenovirus Cre-recombinase (Ad-Cre) to delete the floxed *smoothed* allele.

Conditional deletion of *smoothed* in MF-HSC recapitulated the effects of GDC-0449, causing significant down-regulation of glycolytic genes and MF genes (Fig.3B). Thus, canonical Hh signaling directs HSC transdifferentiation by reprogramming their metabolism. Moreover, our results prove that HSC must maintain Hh signaling in order to retain the glycolytic phenotype of MF, demonstrating that metabolism has a dynamic impact on HSC plasticity.

We next wished to clarify the mechanisms by which Hh directs glycolytic reprogramming. Because HIF1 α is a key regulator of the expression and activity of glycolytic enzymes,³² we mapped changes in HIF1 α expression during HSC transdifferentiation and evaluated the effect of modulating SMO activity. As others have demonstrated,³³ MF-HSC express higher mRNA levels of HIF1 α than Q-HSC. HIF1 α mRNA expression increases significantly within hours of HSC isolation, peaks by day 2 of culture, and remains higher in MF-HSC

than Q-HSC (Fig.3C). Genetic or pharmacologic approaches that inhibited SMO, and suppressed expression of glycolytic and myofibroblastic genes, also inhibited HIF1 α expression. Conversely, activating SMO by SAG treatment up-regulated Hif1 α mRNA expression (Fig.3A-B).

Activated Smoothened promotes nuclear localization and activation of GLIs to control transcription of Hh-regulated genes. We transiently overexpressed GLIs in MF-HSC to see if GLIs regulate HIF1 α . As shown in Fig.3D, compared to MF-HSC transfected with empty vectors, MF-HSC transfected with either GLI1 or GLI2 increased expression of both HIF1 α and HIF1 α target genes. Subsequent analysis of the HIF1 α promoter revealed potential GLI-binding sites, and chromatin immunoprecipitation assays (ChIP) demonstrated that endogenous GLI proteins directly interact with the HIF1 α promoter in MF-HSC (Fig.3F). These results prove that HIF1 α activation is a down-stream consequence of Hh signaling and suggest that the process involves GLI-mediated induction of HIF1 α transcription.

To assure that HIF1 α was the proximal effector of Hh-initiated signals that promoted glycolysis-dependent changes in HSC fate, we then treated MF-HSC with acriflavine (ACF), a direct inhibitor of HIF1 α .²² As expected, treating MF-HSC with the ACF significantly reduced expression of HIF1 α -regulated glycolytic genes, as well as expression of Hh-sensitive cell cycle genes and MF markers, while restoring expression of lipogenic genes towards quiescent levels (Fig.3F). The aggregate results, therefore, demonstrate for the first time that Hh-stimulated HIF1 α expression directs HSC fate.

Metabolic reprogramming of HSC is a conserved response to liver injury

We next studied different animal models of hepatic injury and fibrosis, as well as human liver biopsies, to determine if metabolic reprogramming of HSCs also occurs when HSCs are driven to become MF during liver repair *in vivo*. To assess the effects of acute liver injury, we injected mice with one dose of carbon tetrachloride (CCl₄) and sacrificed them 2, 4, or 7 days later. Hepatocytes around terminal hepatic venules are killed by CCl₄ within 2-3 days, triggering efficient wound healing that results in replacement of the dead hepatocytes by 7 days post-exposure.^{34, 35} We wished to determine if expression of glycolysis-related enzymes changed during an acute wound-healing response. We discovered that hepatic expression of glycolytic enzymes, PDK3, and GLUT1 increased dramatically 2-4 days after CCl₄ injury, the period of maximal hepatocyte death, but declined to near basal levels by day 7, when liver repair was nearly complete. In contrast, expression of the gluconeogenic gene FBP1 declined initially, but then recovered to baseline after hepatocyte regeneration had been accomplished (Fig.4A-B). To localize glycolytic activity during acute liver repair, we performed immunohistochemistry for PKM2, an accepted marker of glycolytic cells.^{27, 36, 37} PKM2(+) cells were scarce in healthy livers but accumulated transiently along sinusoidal spaces of CCl₄-injured livers. Striking accumulation of such cells was evident around terminal hepatic venules in day 4 livers (Fig.4B), coinciding with the peak of hepatocyte death. Conversely, PKM2-expressing cells were no longer evident on day 7, when these damaged areas had been regenerated (Fig.4B). Western blot analysis confirmed that the influx of glycolytic stromal cells occurred in parallel with increased expression of the MF marker, α SMA (Fig.4B). QRT-PCR analysis of whole liver mRNA verified that changes in α SMA protein were matched by changes in α SMA mRNA levels, and accompanied by changes in other MF markers (Collagen1 α 1 and Vimentin) (Supplementary Fig.6A). Double-immunostaining demonstrated co-localization of PKM2 with Desmin, a protein expressed by MF-HSC (Supplementary Fig.7A). Hence, as in the *in vitro* model system (Fig.1), reciprocal changes in glycolytic and gluconeogenic enzymes accompany the outgrowth of MF-HSC during wound healing *in vivo*. The aggregate findings, therefore, are consistent with the concept that HSC undergo rapid metabolic reprogramming during acute liver repair.

To determine if similar metabolic reprogramming also occurs during chronic liver repair, we next examined two mouse models of sustained liver injury and fibrosis: administration of methionine choline-deficient (MCD) diets^{38, 39} (Fig.4C-D) and bile duct ligation^{40, 41} (BDL, Fig.4E-F). When we examined liver tissues from each of these models several weeks after the onset of liver injury, we found that expression of glycolytic enzymes and GLUT1 had increased significantly, while expression of FBP1 was suppressed (Fig.4C-F). Western blot and QRT-PCR analysis demonstrated that these changes in metabolic gene expression consistently paralleled the induction of MF markers (Fig.4D, F, Supplementary Fig.6B-C). PKM2 expression was also localized by immunohistochemistry. The results confirmed that like acute liver repair (Fig.4B), repair of chronic damage to either bile ducts (Fig.4D) or hepatocytes (Fig.4F) causes accumulation of PKM2(+) stromal cells, and these PKM2(+) stromal cells co-express Desmin (Supplementary Fig.7).

To assure that findings in the animal models of fatty liver damage and cholestatic liver injury reliably reflected responses that occur in humans with similar injuries, we compared expression of glycolytic enzymes in liver biopsies from subjects without known liver disease to that of patients with chronic hepatocyte or biliary injury. Compared to healthy subjects, patients with liver disease expressed higher mRNA levels of glycolytic enzymes and demonstrated relative accumulation of glycolytic stromal cells (Supplementary Fig.4A-B). Sufficient biopsy material was available from the group of NASH patients to determine if glycolytic activity correlated with the intensity of fibrotic repair. Patients with more severe liver fibrosis had higher expression of PKM2 than patients with less severe fibrosis (Supplementary Fig.4C), supporting the concept that metabolic reprogramming drives the generation of fibrogenic cells. Thus, during different types and durations of liver injury in rodents and humans, repair-related outgrowth of MF is tightly coupled to increased glycolytic activity and relative suppression of gluconeogenic activity, supporting the concept that metabolic reprogramming of HSC is a strictly conserved aspect of liver repair.

Hh signaling controls metabolic reprogramming during liver repair

Finally, to verify that Hh signaling controls metabolic reprogramming of HSC *in vivo*, as it does *in vitro*, we manipulated Hh signaling in mice with different types of liver injury and assessed effects on the hepatic accumulation of stromal cells expressing the glycolysis marker, PKM2. The livers of healthy adult mice harbored very few PKM2(+) cells (Fig.5A). In contrast, marked sinusoidal accumulation of PKM2-expressing cells was observed in previously healthy mice when liver repair was provoked by acute two-thirds (partial) hepatectomy (PH) (Fig.5B), a surgical insult that triggers transient MF accumulation and matrix remodeling.^{23, 42-44} Extensive sinusoidal accumulation of PKM2(+) cells was also noted in transgenic multi-drug resistant (MDR)2 knockout mice (Fig.5C) which chronically accumulate large numbers of liver MF and develop progressive liver fibrosis due to persistent liver injury caused by targeted disruption of the gene encoding the phospholipid flippase, MDR2.⁴⁵ In both models, PKM2 was localized within stromal cells that expressed Desmin (Supplementary Fig.7). Pharmacologic SMO inhibition in both models of injury significantly decreased PKM2(+) stromal cells. Specifically, administering cyclopamine during the first two days post-PH blocked the accumulation of PKM2(+) cells (Fig.5B). To exclude the possibility that decreased glycolytic activity might have resulted from off-target effects of cyclopamine and/or unrecognized dissipation of signals that normally drive acute repair responses, we examined the effect of a different Hh pathway inhibitor in a model of perpetual, genetically-induced liver damage. We found that treating year-old MDR2^{-/-} mice with a 9-day course of GDC-0449²⁴ substantially reduced the numbers of PKM2(+) cells despite the ongoing genetic stimulus for liver repair (Fig.5C). Because the aggregate *in vivo* data recapitulated our findings in cultured HSC, the latter cannot be dismissed as a mere

artifact of cell culture. Rather, both the *in vitro* and *in vivo* results show that Hh pathway activity critically regulates HSC metabolism.

Pharmacologic inhibition of Hh signaling blocked MF accumulation and reduced liver fibrosis in the PH and MDR2^{-/-} mice models.^{23, 24} The data in Fig.4 link MF accumulation and fibrogenic repair with induction of glycolysis in MF-HSC. Disruption of the Smo gene in cultured MF-HSC reverted them to a quiescent, non-fibrogenic state (Fig.3). Therefore, to directly examine the effect of Hh signaling on MF-HSC metabolism *in situ*, we created double-transgenic (DTG) mice by crossing SMO-LoxP mice with α SMA-Cre-ERT2 mice, the latter animals carrying regulatory elements of α SMA that control expression of the tamoxifen-dependent Cre-ERT2 recombinase Cre. In DTG mice, floxed SMO alleles can be conditionally and selectively deleted in MF by administering tamoxifen (*Michelotti et al, manuscript under review*). When DTG mice were subjected to BDL and treated with vehicle, large numbers of PKM2(+) stromal cells accumulated (Fig.5D). Similar to wild-type mice subjected to the same insult, the PKM2(+) stromal cells in DTG mice co-expressed Desmin (Supplementary Fig.7). In contrast, PKM2(+) stromal cells were scarce in the livers of DTG mice treated with tamoxifen post-BDL (Fig.5D, Supplementary Fig. 7). Whole liver mRNA levels of α SMA, another well-accepted marker of MF-HSC,² were also reduced by more than 85% and immunocytochemistry demonstrated similar reductions in numbers α SMA-expressing cells. MF depletion was accompanied by significant attenuation of collagen gene expression and hepatic hydroxyproline content (all $p < 0.05$ vs vehicle-treated DTG mice; *Michelotti et al, manuscript under review*). Thus, targeting deletion of SMO to MF in conditional knockout mice proved that inhibiting Hh signaling in MF prevents accumulation of glycolytic, fibrogenic MF-HSC *in situ* despite an ongoing stimulus for liver repair.

Discussion

We have identified a novel mechanism for reprogramming Q-HSC into MF that depends upon induction of aerobic glycolysis, similar to the Warburg state described in cancer cells.^{26, 28} Moreover, we have proven that this metabolic switch is regulated by the Hedgehog pathway. Hedgehog signaling was shown to direct preferential induction of a metabolic process (glycolysis) that consumes glucose, while coincidentally suppressing gluconeogenesis and lipogenesis. As a result of these metabolic perturbations, HSC accumulate lactate and the latter metabolite re-enforces global reprogramming of their gene expression to activate key fates that typify MF, including high proliferative and fibrogenic activities (Fig.6). This metabolism-centric mechanism is both dynamic and robust, rapidly affecting dramatic phenotypic changes in HSC that titrate MF accumulation during liver repair. These findings lend new credence to the old adage, “you are what you eat”.

Hedgehog is an evolutionarily conserved signaling pathway that directs organogenesis and controls body size. Interactions between Hh and other key developmental signaling cascades, such as Notch and Wnt, have been well-documented,^{21, 46, 47} suggesting that these pathways collaborate to assure that morphogenesis matches the environmental context. A similar demand re-surfaces in adulthood when damage to vital tissues necessitates regeneration to reconstitute lost tissue-specific functions. Studies of wound-healing responses in injured adult liver demonstrate that Hh ligands function as damage-associated molecular signals to trigger repair of the damaged hepatic epithelia.⁵ Dying hepatocytes produce and release Hh ligands, which activate Hh signaling in neighboring Hh-responsive stromal cells.⁴⁸ The latter include all of the resident cell types that are involved in liver repair, including HSC, sinusoidal endothelial cells, immune cells, and progenitors.¹⁰ The current study focused on HSC, which have been shown to become proliferative and myofibroblastic in response to Hh pathway activation.^{13, 18, 49} We found that Hh affects this

dramatic phenotypic transition by reprogramming HSC metabolism, and showed that Hh signaling orchestrates reprogramming by directing the activation of HIF1 α , another stress-related transcriptional regulator that is known to promote fibrogenesis.^{50, 51} Earlier work demonstrated that activation of canonical Hh signaling results when various fibrogenic growth factors interact with their respective receptors.^{18, 19} Thus, emerging evidence supports the existence of a novel Hh-regulated signaling network that is triggered when circumstances dictate expansion of relatively mesenchymal cell types. According to this model, the network fuels the outgrowth of highly proliferative, but relatively primitive, stromal cells by redirecting their metabolism to optimize glucose consumption. The same process limits accumulation of more differentiated and quiescent cell types. This concept has broad biological relevance, as well as potential therapeutic implications for various diseases that result from deregulated Hh signaling, including cirrhosis and liver cancer.

Supplementary Material

Refer to Web version on PubMed Central for supplementary material.

Acknowledgments

This work was supported in part by grants R37 AA010154 and R01 DK077794 (AMD)

References

1. Tsukamoto H. Adipogenic phenotype of hepatic stellate cells. *Alcohol Clin Exp Res.* 2005; 29:132S–133S. [PubMed: 16344597]
2. Friedman SL. Hepatic stellate cells: protean, multifunctional, and enigmatic cells of the liver. *Physiol Rev.* 2008; 88:125–72. [PubMed: 18195085]
3. Jiang J, Hui CC. Hedgehog signaling in development and cancer. *Dev Cell.* 2008; 15:801–12. [PubMed: 19081070]
4. Ribes V, Briscoe J. Establishing and interpreting graded Sonic Hedgehog signaling during vertebrate neural tube patterning: the role of negative feedback. *Cold Spring Harb Perspect Biol.* 2009; 1:a002014. [PubMed: 20066087]
5. Omenetti A, Choi S, Michelotti G, et al. Hedgehog signaling in the liver. *J Hepatol.* 2011; 54:366–73. [PubMed: 21093090]
6. Hui CC, Angers S. Gli proteins in development and disease. *Annu Rev Cell Dev Biol.* 2011; 27:513–37. [PubMed: 21801010]
7. Stecca B, Ruiz I A A. Context-dependent regulation of the GLI code in cancer by HEDGEHOG and non-HEDGEHOG signals. *J Mol Cell Biol.* 2010; 2:84–95. [PubMed: 20083481]
8. Zhu H, Lo HW. The Human Glioma-Associated Oncogene Homolog 1 (GLI1) Family of Transcription Factors in Gene Regulation and Diseases. *Curr Genomics.* 11:238–45. [PubMed: 21119888]
9. Barakat MT, Humke EW, Scott MP. Learning from Jekyll to control Hyde: Hedgehog signaling in development and cancer. *Trends Mol Med.* 2010; 16:337–48. [PubMed: 20696410]
10. Choi SS, Bradrick S, Qiang G, et al. Upregulation of Hedgehog pathway is associated with cellular permissiveness for hepatitis C virus. *Hepatology.* 2011; 25
11. Pospisilik JA, Schramek D, Schnidar H, et al. *Drosophila* genome-wide obesity screen reveals hedgehog as a determinant of brown versus white adipose cell fate. *Cell.* 2010; 140:148–60. [PubMed: 20074523]
12. Beachy PA, Karhadkar SS, Berman DM. Tissue repair and stem cell renewal in carcinogenesis. *Nature.* 2004; 432:324–31. [PubMed: 15549094]
13. Choi SS, Omenetti A, Witek RP, et al. Hedgehog pathway activation and epithelial-to-mesenchymal transitions during myofibroblastic transformation of rat hepatic cells in culture and cirrhosis. *Am J Physiol Gastrointest Liver Physiol.* 2009; 297:G1093–106. [PubMed: 19815628]

14. Lee TF, Mak KM, Rackovsky O, et al. Downregulation of hepatic stellate cell activation by retinol and palmitate mediated by adipose differentiation-related protein (ADRP). *J Cell Physiol.* 2010; 223:648–57. [PubMed: 20143336]
15. Kluwe J, Wongsiriroj N, Troeger JS, et al. Absence of hepatic stellate cell retinoid lipid droplets does not enhance hepatic fibrosis but decreases hepatic carcinogenesis. *Gut.* 2011
16. Long F, Zhang XM, Karp S, et al. Genetic manipulation of hedgehog signaling in the endochondral skeleton reveals a direct role in the regulation of chondrocyte proliferation. *Development.* 2001; 128:5099–108. [PubMed: 11748145]
17. Shitara H, Kaneda H, Sato A, et al. Non-invasive visualization of sperm mitochondria behavior in transgenic mice with introduced green fluorescent protein (GFP). *FEBS Lett.* 2001; 500:7–11. [PubMed: 11434917]
18. Yang L, Wang Y, Mao H, et al. Sonic hedgehog is an autocrine viability factor for myofibroblastic hepatic stellate cells. *J Hepatol.* 2008; 48:98–106. [PubMed: 18022723]
19. Choi SS, Syn WK, Karaca GF, et al. Leptin promotes the myofibroblastic phenotype in hepatic stellate cells by activating the hedgehog pathway. *J Biol Chem.* 2010; 285:36551–60. [PubMed: 20843817]
20. Le A, Cooper CR, Gouw AM, et al. Inhibition of lactate dehydrogenase A induces oxidative stress and inhibits tumor progression. *Proc Natl Acad Sci U S A.* 2010; 107:2037–42. [PubMed: 20133848]
21. Toku AE, Tekir SD, Ozbayraktar FB, et al. Reconstruction and crosstalk of protein-protein interaction networks of Wnt and Hedgehog signaling in *Drosophila melanogaster*. *Comput Biol Chem.* 2011; 35:282–92. [PubMed: 22000799]
22. Lee K, Zhang H, Qian DZ, et al. Acriflavine inhibits HIF-1 dimerization, tumor growth, and vascularization. *Proc Natl Acad Sci U S A.* 2009; 106:17910–5. [PubMed: 19805192]
23. Ochoa B, Syn WK, Delgado I, et al. Hedgehog signaling is critical for normal liver regeneration after partial hepatectomy in mice. *Hepatology.* 2010; 51:1712–23. [PubMed: 20432255]
24. Philips GM, Chan IS, Swiderska M, et al. Hedgehog signaling antagonist promotes regression of both liver fibrosis and hepatocellular carcinoma in a murine model of primary liver cancer. *PLoS One.* 2011; 6:e2393.
25. De Minicis S, Seki E, Uchinami H, et al. Gene expression profiles during hepatic stellate cell activation in culture and in vivo. *Gastroenterology.* 2007; 132:1937–46. [PubMed: 17484886]
26. Vander Heiden MG, Cantley LC, Thompson CB. Understanding the Warburg effect: the metabolic requirements of cell proliferation. *Science.* 2009; 324:1029–33. [PubMed: 19460998]
27. Sun Q, Chen X, Ma J, et al. Mammalian target of rapamycin up-regulation of pyruvate kinase isoenzyme type M2 is critical for aerobic glycolysis and tumor growth. *Proc Natl Acad Sci U S A.* 2006; 66:8927–30. [PubMed: 16982728]
28. Kim JW, Dang CV. Cancer's molecular sweet tooth and the Warburg effect. *Cancer Res.* 2006; 66:8927–30. [PubMed: 16982728]
29. Ramanathan A, Wang C, Schreiber SL. Perturbational profiling of a cell-line model of tumorigenesis by using metabolic measurements. *Proc Natl Acad Sci U S A.* 2005; 102:5992–7. [PubMed: 15840712]
30. Chen JK, Taipale J, Young KE, et al. Small molecule modulation of Smoothed activity. *Proc Natl Acad Sci U S A.* 2002; 99:14071–6. [PubMed: 12391318]
31. Rominger CM, Bee WL, Copeland RA, et al. Evidence for allosteric interactions of antagonist binding to the smoothed receptor. *J Pharmacol Exp Ther.* 2009; 329:995–1005. [PubMed: 19304771]
32. Semenza GL, Roth PH, Fang HM, et al. Transcriptional regulation of genes encoding glycolytic enzymes by hypoxia-inducible factor 1. *J Biol Chem.* 1994; 269:23757–63. [PubMed: 8089148]
33. Shi YF, Fong CC, Zhang Q, et al. Hypoxia induces the activation of human hepatic stellate cells LX-2 through TGF-beta signaling pathway. *FEBS Lett.* 2007; 581:203–10. [PubMed: 17187782]
34. Bezerra JA, Bugge TH, Melin-Aldana H, et al. Plasminogen deficiency leads to impaired remodeling after a toxic injury to the liver. *Proc Natl Acad Sci U S A.* 1999; 96:15143–8. [PubMed: 10611352]
35. Mehendale HM. Tissue repair: an important determinant of final outcome of toxicant-induced injury. *Toxicol Pathol.* 2005; 33:41–51. [PubMed: 15805055]

36. Christofk HR, Vander Heiden MG, Harris MH, et al. The M2 splice isoform of pyruvate kinase is important for cancer metabolism and tumour growth. *Nature*. 2008; 452:230–3. [PubMed: 18337823]
37. Hitosugi T, Kang S, Vander Heiden MG, et al. Tyrosine phosphorylation inhibits PKM2 to promote the Warburg effect and tumor growth. *Sci Signal*. 2009; 2:ra73. [PubMed: 19920251]
38. Soon RK Jr, Yan JS, Grenert JP, et al. Stress signaling in the methionine-choline-deficient model of murine fatty liver disease. *Gastroenterology*. 2010; 139:1730–9. 1739 e1. [PubMed: 20682321]
39. Caballero F, Fernandez A, Matias N, et al. Specific contribution of methionine and choline in nutritional nonalcoholic steatohepatitis: impact on mitochondrial S-adenosyl-L-methionine and glutathione. *J Biol Chem*. 2010; 285:18528–36. [PubMed: 20395294]
40. Uchinami H, Seki E, Brenner DA, et al. Loss of MMP 13 attenuates murine hepatic injury and fibrosis during cholestasis. *Hepatology*. 2006; 44:420–9. [PubMed: 16871591]
41. Takeda K, Kojima Y, Ikejima K, et al. Death receptor 5 mediated-apoptosis contributes to cholestatic liver disease. *Proc Natl Acad Sci U S A*. 2008; 105:10895–900. [PubMed: 18667695]
42. Rudolph KL, Trautwein C, Kubicka S, et al. Differential regulation of extracellular matrix synthesis during liver regeneration after partial hepatectomy in rats. *Hepatology*. 1999; 30:1159–66. [PubMed: 10534336]
43. Wack KE, Ross MA, Zegarra V, et al. Sinusoidal ultrastructure evaluated during the revascularization of regenerating rat liver. *Hepatology*. 2001; 33:363–78. [PubMed: 11172338]
44. Yamamoto H, Murawaki Y, Kawasaki H. Hepatic collagen synthesis and degradation during liver regeneration after partial hepatectomy. *Hepatology*. 1995; 21:155–61. [PubMed: 7806150]
45. Igolnikov AC, Green RM. Mice heterozygous for the Mdr2 gene demonstrate decreased PEMT activity and diminished steatohepatitis on the MCD diet. *J Hepatol*. 2006; 44:586–92. [PubMed: 16376450]
46. Katoh Y, Katoh M. Integrative genomic analyses on GLI1: positive regulation of GLI1 by Hedgehog-GLI, TGFbeta-Smads, and RTK-PI3K-AKT signals, and negative regulation of GLI1 by Notch-CSL-HES/HEY, and GPCR-Gs-PKA signals. *Int J Oncol*. 2009; 35:187–92. [PubMed: 19513567]
47. Roldan M, Macias-Gonzalez M, Garcia R, et al. Obesity short-circuits stemness gene network in human adipose multipotent stem cells. *FASEB J*. 2011; 25:4111–26. [PubMed: 21846837]
48. Jung Y, Witek RP, Syn WK, et al. Signals from dying hepatocytes trigger growth of liver progenitors. *Gut*. 2010; 59:655–65. [PubMed: 20427400]
49. Sicklick JK, Li YX, Choi SS, et al. Role for hedgehog signaling in hepatic stellate cell activation and viability. *Lab Invest*. 2005; 85:1368–80. [PubMed: 16170335]
50. Moon JO, Welch TP, Gonzalez FJ, et al. Reduced liver fibrosis in hypoxia-inducible factor-1alpha-deficient mice. *Am J Physiol Gastrointest Liver Physiol*. 2009; 296:G582–92. [PubMed: 19136383]
51. Higgins DF, Kimura K, Bernhardt WM, et al. Hypoxia promotes fibrogenesis in vivo via HIF-1 stimulation of epithelial-to-mesenchymal transition. *J Clin Invest*. 2007; 117:3810–20. [PubMed: 18037992]

Abbreviations

Ad	adenovirus
ACF	acriflavine
αSMA	α smooth muscle actin
BDL	bile duct ligation
CCl₄	carbon tetrachloride
CCNB1 & 2	cyclin B1 & 2
COL1α1	collagen type I, α1

CRE	Cre recombinase
2DG	2 deoxy-D-glucose
ENO1 & 2	enolase 1 & 2
FBP1	fructose bisphosphatase 1
FOXM1	forkhead box M1
GFP	green fluorescent protein
Gli	glioblastoma
GLUT1	glucose transporter 1
Hh	Hedgehog
HIF1α	hypoxia inducible factor 1 α
HK2	hexokinase 2
HSC	hepatic stellate cell
MCD	methionine-choline-deficient
MCT4	lactate transporter 4
MDR2	the murine ortholog of MDR3
MF	myofibroblast
PCK1	phosphoenolpyruvate carboxykinase 1
PDK3	Pyruvate dehydrogenase kinase 3
PFKP	phosphofructokinase platelet
PGAM1	phosphoglycerate mutase 1
PGK1	phosphoglycerate kinase 1
PH	partial hepatectomy
PKM2	pyruvate kinase M2
PPARα & γ	peroxisome proliferator-activated receptor α & γ
PTCH	Patched
Q-HSC	quiescent hepatic stellate cell
S100A4	S100 calcium binding protein A4
SMO	smoothened
VIM	vimentin

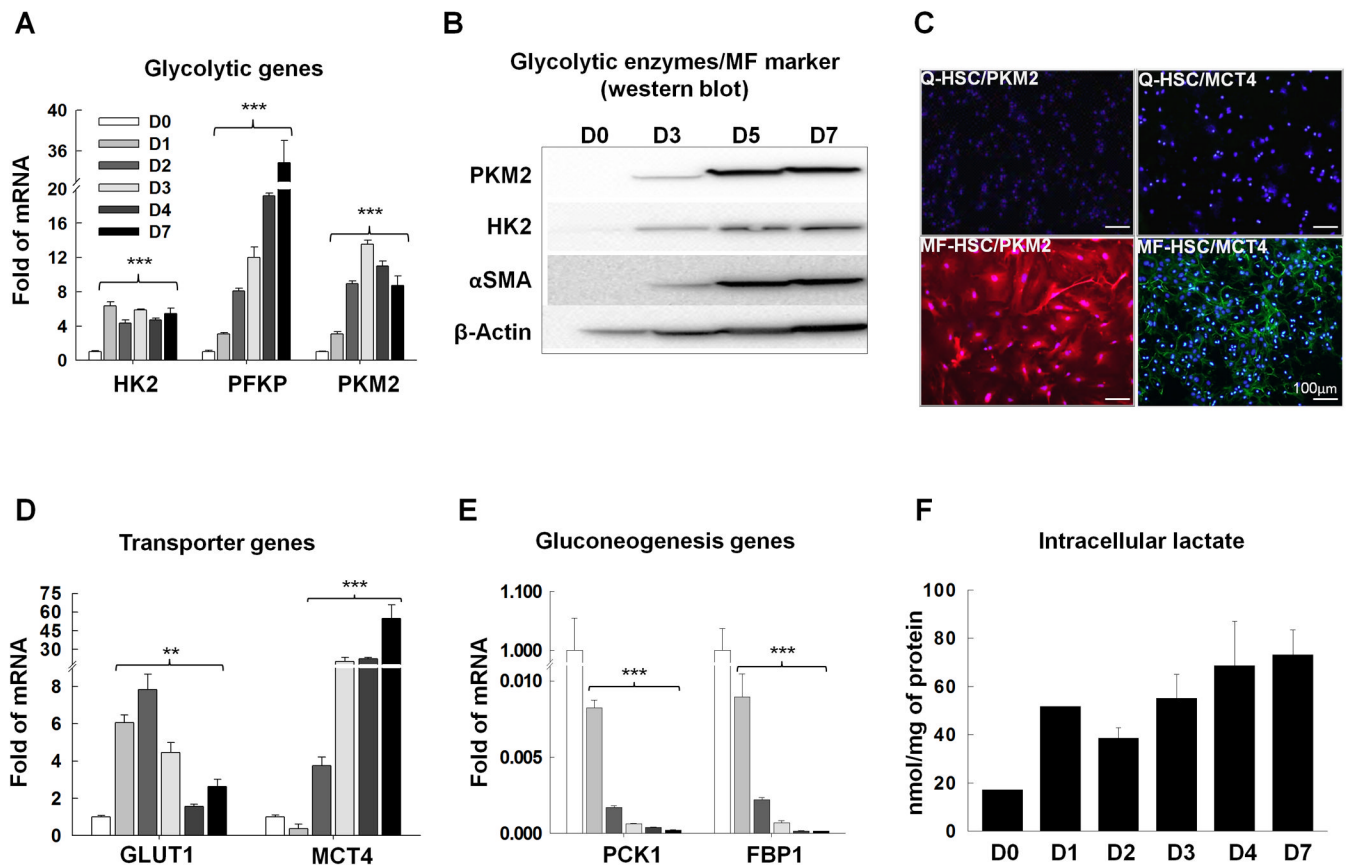


Figure 1. Metabolism is reprogrammed during HSC transdifferentiation

Primary HSCs were cultured for 7 days. Culture-related changes in *A*) mRNA and *B, C*) protein expression of glycolytic enzymes, hexokinase (HK2), phosphofruktokinase (PFKP), and pyruvate kinase M2 (PKM2). Related changes in *B*) the MF marker (α SMA), *D*) glucose transporter (GLUT1), lactate transporter (MCT4), *E*) gluconeogenesis-related genes, phosphoenolpyruvate carboxykinase (PCK1) and fructose bisphosphatase (FBP1), and *F*) intracellular lactate. * $P < .05$; ** $P < .01$; *** $P < .001$ versus day 0.

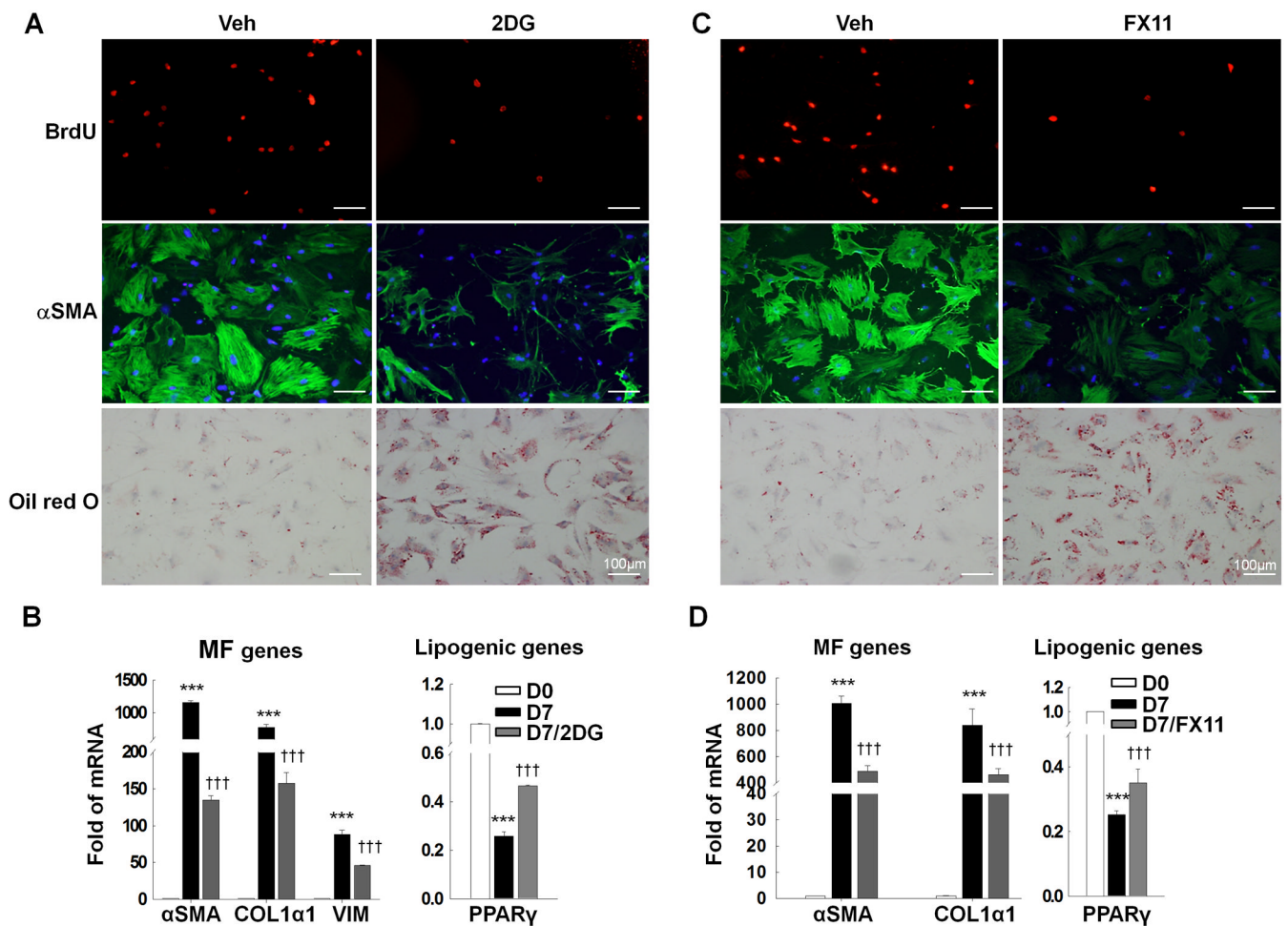


Figure 2. Metabolic reprogramming controls the fate of HSCs

Seven-day cultured primary HSCs were analyzed after three-days of treatment with 2-deoxyglucose (2DG, 2.5mM) to inhibit glycolysis (A, B) or FX11 (20 μ M, LDHA inhibitor) to block lactate generation (C, D). Immunocytochemistry was used to compare effects of 2DG (A) or FX11 (C) on proliferation (BrdU incorporation), expression of MF markers (α SMA), and lipid content (Oil red O). B, D) Changes in gene expression were assessed by QRT-PCR. *** P <.001 versus Day 0; ††† P <.001 versus Day 7 control.

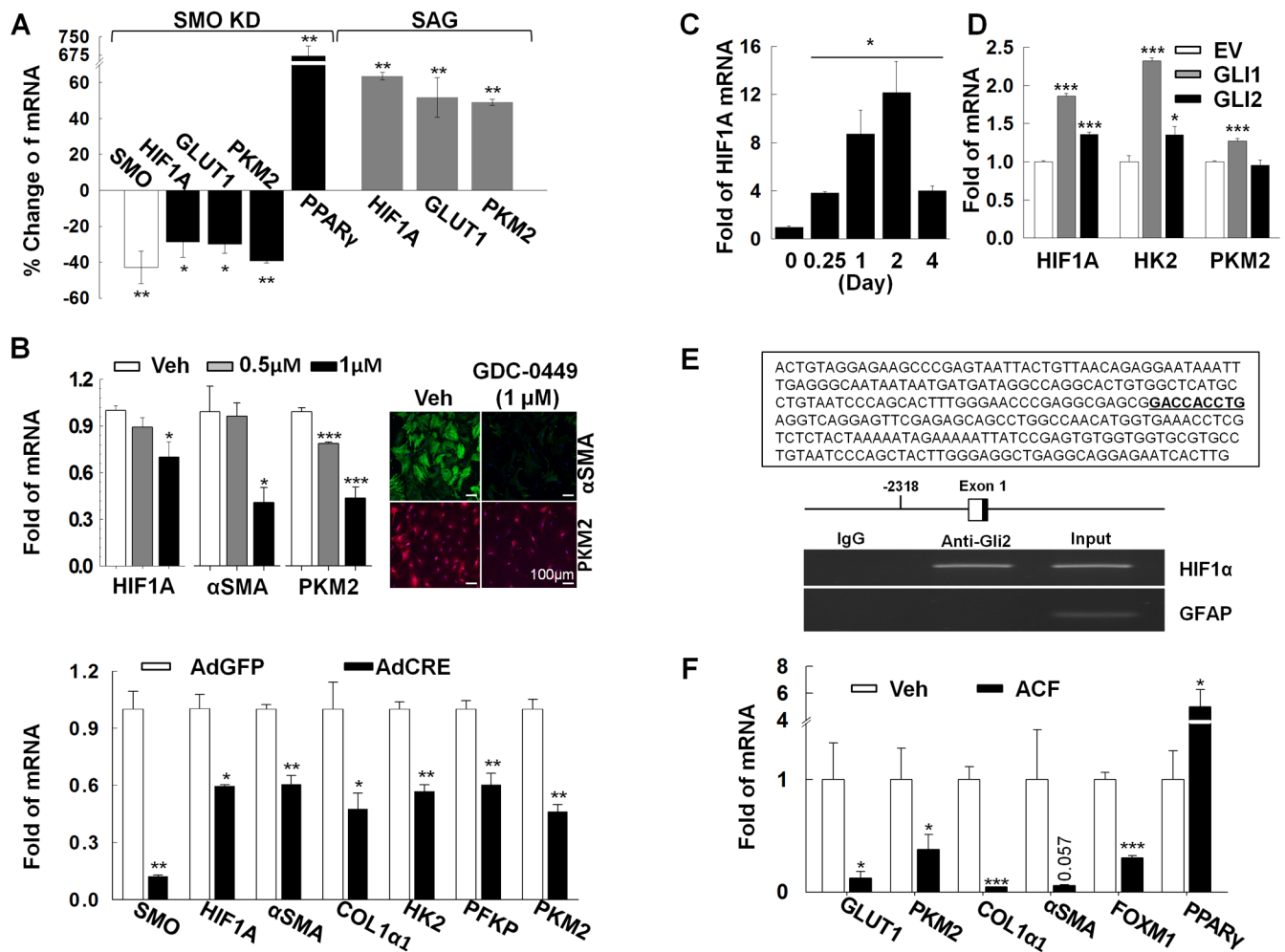


Figure 3. Hedgehog signaling controls metabolic reprogramming to direct HSC fate

A) QRT-PCR analysis of freshly-isolated HSCs from SMO-LoxP mice that were infected with adenoviral GFP or Cre 2-days before HSC isolation, and freshly-isolated rat primary HSC treated with SAG (Hh agonist, 0.3μM) for 24 hours; B) QRT-PCR analysis and immunostaining of murine HSC treated with GDC-0449 (to inhibit SMO) from culture day 4-7, or culture day 7 SMO-LoxP HSC treated with adenoviral Cre on day 4 (to disrupt the Smo gene); C) QRT-PCR analysis of HIF1α mRNA in primary rat HSC and D) 8B cells transfected with equal amounts of expression constructs for GLI1 or GLI2 (or empty vector) 2 days earlier; E) Chromatin was immunoprecipitated from LX2 cells using GLI2 or IgG antibodies and analyzed by PCR. The GLI consensus sequence within the ChIP amplicon is bolded and underlined. GFAP was used as a specificity control. F), QRT-PCR analysis of culture-day 7 HSCs treated with acriflavine (ACF, HIF1α inhibitor) for three days. * $P < .05$; ** $P < .01$; *** $P < .001$ versus control.

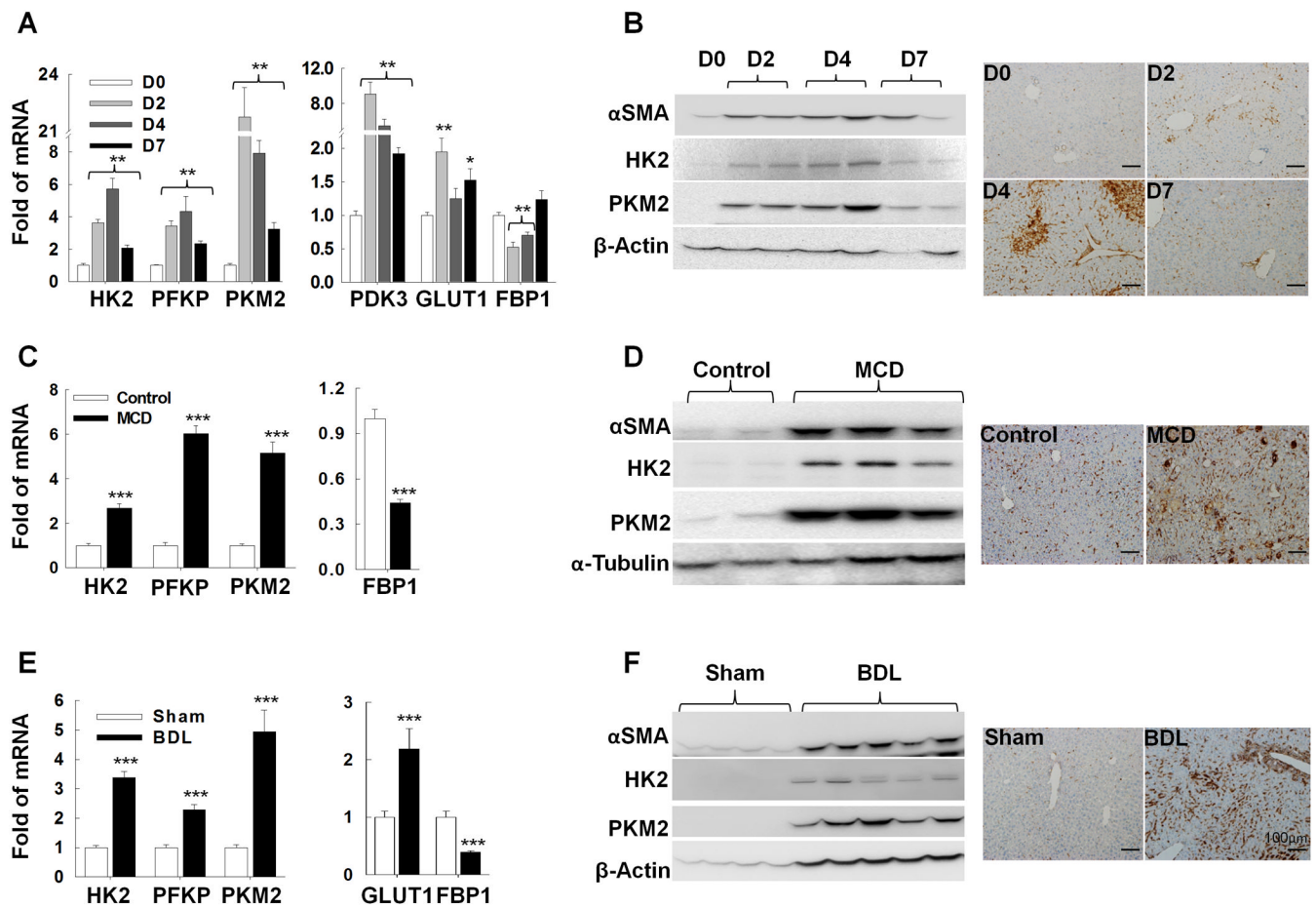


Figure 4. Metabolic reprogramming of HSCs is a conserved response to liver injury
Mice injected once with CCl₄ (A, B), fed methionine-choline deficient (MCD) diets for 8 weeks (C, D) or subjected to bile duct ligation (BDL, E, F) for 2 weeks to cause liver damage. Changes in glycolysis-related gene/protein expression were evaluated by QRT-PCR (A, C, E), immunoblot and immunohistochemistry (B, D, F) and correlated with changes in MF marker expression (B, D, F and Supplementary Fig.3). * $P < .05$; ** $P < .01$; *** $P < .001$ versus control.

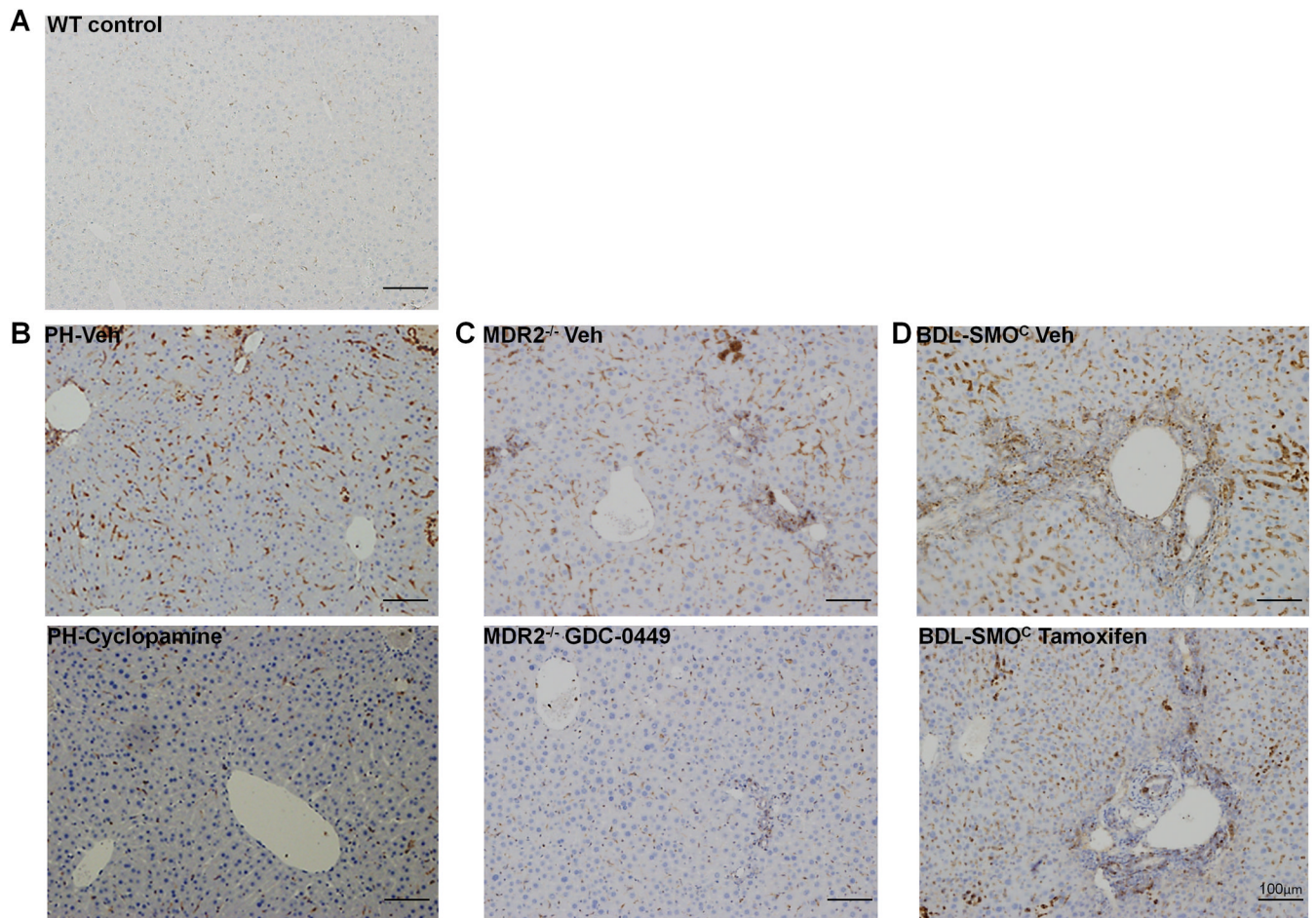


Figure 5. Hedgehog signaling controls metabolic reprogramming during liver injury *in vivo*
 Immunohistochemistry identifies cells expressing the M2 isozyme of PKM2, a specific marker of glycolytic activity, in healthy adult mice (A) and different liver injury models (B-D). Hh signaling was inhibited in PH-mice by cyclopamine (B), in aged MDR2^{-/-} mice by GDC-0449 (C), or abrogated selectively in MF by treating DTG-mice with tamoxifen (D), as indicated.

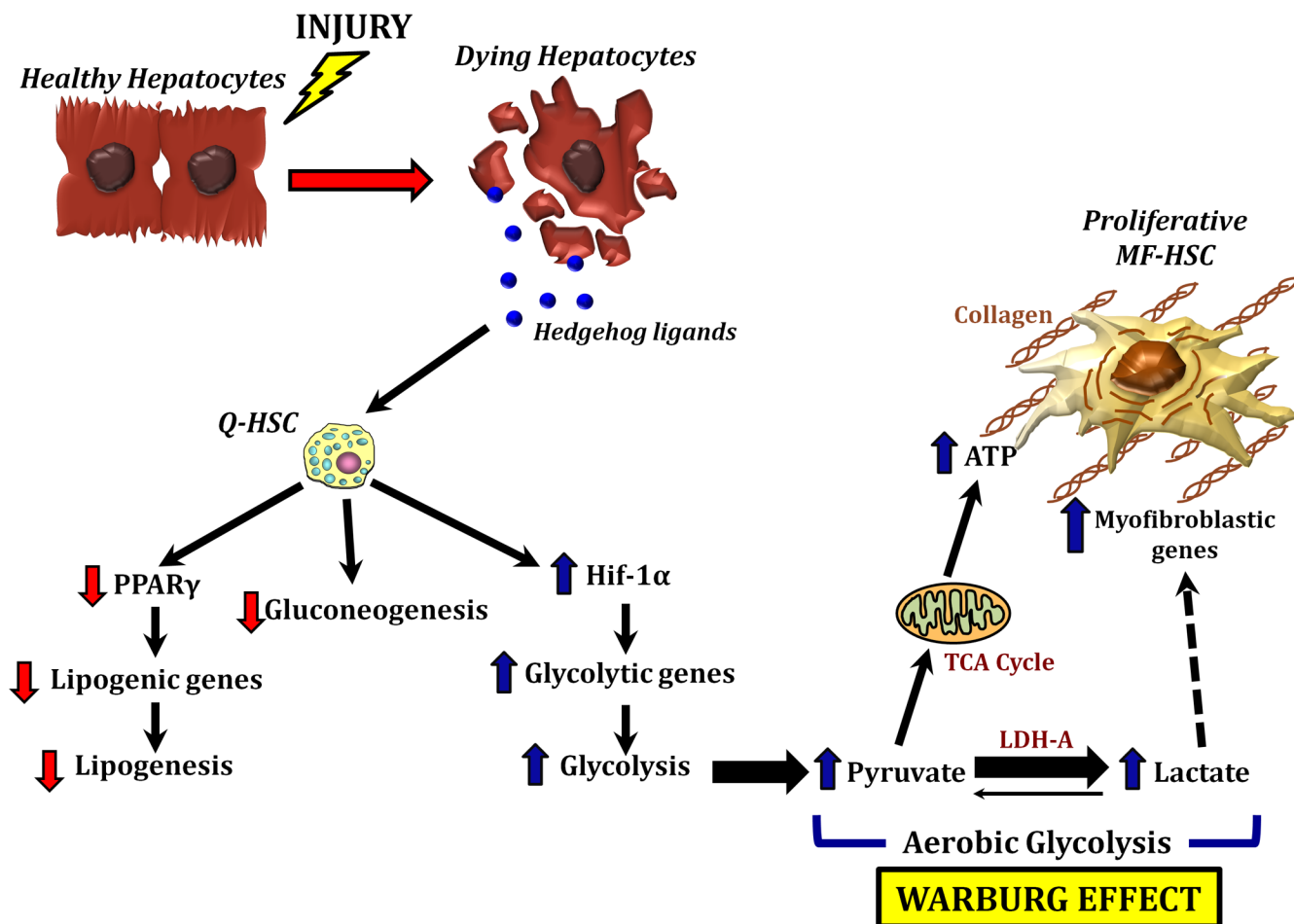


Figure 6. Hedgehog controls HSC fate by regulating metabolism

Hh ligands released from dying hepatocytes activate Hh signaling in Q-HSC. This inhibits lipogenesis and gluconeogenesis while activating aerobic glycolysis (the Warburg effect). The resultant glycolytic end-products reprogram HSC into proliferative myofibroblasts.